

Alignment analysis of four-mirror spherical aberration correctors

Anastacia M. Hvisc*, James H. Burge
College of Optical Sciences/The University of Arizona
1630 East University Boulevard, Tucson, AZ, USA 85721-0094

ABSTRACT

Telescopes use primary mirrors with spherical shape to reduce the cost of the mirror fabrication and to allow the mirror to operate at fixed elevation. These advantages become significant as the size of the telescope grows. However, the disadvantage of the spherical primary is a large amount of spherical aberration which needs to be corrected. We present an analysis of alignment issues for four-mirror spherical aberration correctors for spherical primary mirror telescopes. The sensitivities of image quality across the field (in terms of spot size) to mirror misalignments are found. These sensitivities are useful in choosing the tolerances for the mechanical assembly holding the corrector. A singular value decomposition of the sensitivity matrix shows the combination of element motions that result in orthogonal aberration modes. Studying these combinations of modes and misalignments can lead to a conceptual understanding of the system, which aids in the initial and operational alignment of the spherical aberration corrector.

Keywords: Telescopes, Alignment, Aberrations, Tolerancing, Zernike polynomials, SVD

1. INTRODUCTION

Two examples of telescopes with spherical primary mirrors are the Hobby-Eberly Telescope (HET)¹⁻³ and the Southern African Large Telescope (SALT).⁴⁻⁶ SALT is designed as a southern hemisphere second generation version of the HET. These are both operational ~10 meter class segmented primary mirror optical telescopes. One advantage of a spherical primary mirror telescope is easier primary mirror fabrication. Another benefit is that they allow a fixed elevation mounting scheme. Since the primary mirror does not need to move with respect to gravity, the mirror deformation due to gravity does not change. These advantages become significant as the size of the telescope grows. Larger telescopes that use fixed elevation spherical primary mirrors, such as the Overwhelmingly Large Telescope (OWL),⁷ have been considered. Fixed elevation spherical primary mirror designs are not exclusive to optical telescopes; Arecibo, a radio telescope, uses this technique as well.

1.1 Corrector design

A single reflection from a spherical mirror causes spherical aberration, which is constant across the field, and coma, which is linear across the field. If any field is desired, then a corrector must be used to minimize the aberration. HET currently uses a two-mirror corrector for spherical aberration which has a 4 arcminute diameter field of view. To achieve a wider field of view, SALT chose to adopt a four-mirror corrector instead. This four-mirror system is called the Spherical Aberration Corrector (SAC) and is designed for an 8 arcminute diameter field of view. Currently, HET is planning a major upgrade which includes a new four-mirror corrector called the Wide Field Corrector (WFC). The HET WFC (see Figure 1) is modeled after the SALT corrector, but was modified to increase the field of view to 22 arcminutes (science field of 18 arcminutes). To increase the field of view by such a large amount, the size of the corrector needs to grow (both in length and individual mirror diameters) and the aspheric departure for each of the four mirrors in the WFC significantly increases.

*amh21@email.arizona.edu; phone (520) 626-0486

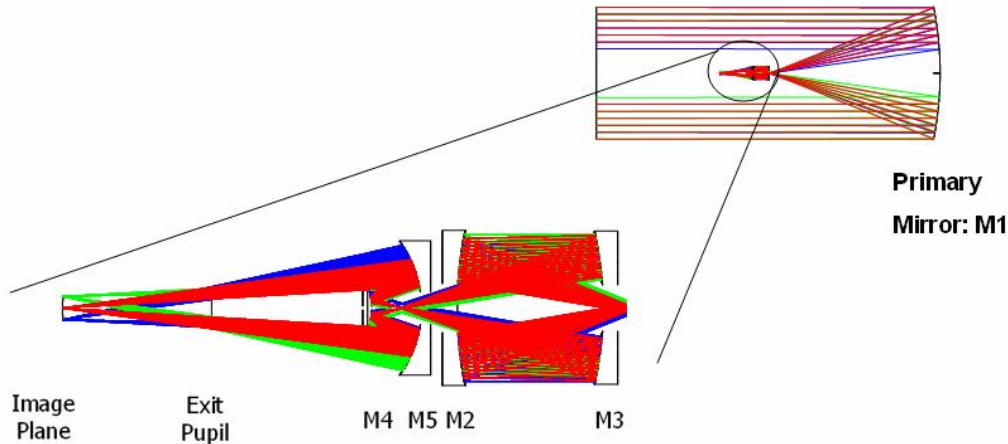


Fig. 1. The optical layout of the Wide Field Corrector for the Hobby-Eberly Telescope. The focus of the primary mirror lies near the central hole of M3. The design of the Spherical Aberration Corrector for SALT looks similar.

1.2 Alignment of the corrector

The desired image quality across the field requires proper alignment of all four mirrors in the corrector. Misalignments result in a degradation of image quality due to field-dependent aberrations. In this paper, we discuss both finding alignment sensitivities to spot size and the orthogonal field-dependent aberration modes that such a system is capable of producing. A spot size sensitivity analysis to mirror misalignments is helpful while choosing mechanical tolerances. But, it does not help aid in understanding the field dependence of the aberrations that the misalignments cause. However, a singular value decomposition (SVD) of the sensitivity matrix describes the orthogonal aberrations that the system may produce and which combinations of mirror motions cause these aberrations.

2. SENSITIVITY ANALYSIS

Before fabricating an optical system, a budget should be made to account for all sources of degradation to the image quality. Tolerances must be specified to ensure that the built system will perform as desired. Tolerances may be specified for the optical surfaces (for example, for radii of curvature, conic constants, rms surface error or even errors in the optical test) or for the mechanics of the system (including mirror deformations and rigid body misalignments). A sensitivity analysis is an important step in the design process because it allows the tolerances to be chosen intelligently. One should only choose tight tolerances when absolutely necessary.

The tolerancing procedure was divided into three main steps, using the HET WFC as an example. The first step was a perturbation analysis to determine the sensitivities. This section will focus on describing the sensitivities specifically related to the optical alignment. The second step was to assign tolerances based on the sensitivities calculated in step 1 and prior experience with similar mechanical designs. The final step was a Monte Carlo analysis to estimate statistics resulting from the chosen tolerances to verify that the system is expected to meet all specifications.

2.1 Finding the sensitivities

The sensitivity analysis determines the effect of small deviations in the system parameters, such as misalignments, on the system performance metric. Wavefront error and spot size are both common performance metrics in optical systems. We use a field averaged rms spot size as the performance criteria in this sensitivity analysis. The field weighted rms spot size was calculated in Zemax using the default merit function for rms spot radius with respect to the centroid for five field points: one zero field point and four at $(\pm 5, \pm 5)$ arcminutes. The performance metric is a function of multiple parameters x_i in the system. For example, a change in one of these variables, such as a misalignment, changes the performance from $\Phi(x_i)$ to a new value $\Phi(x_i + \Delta x_i)$. Assuming that the sources of all the errors are uncorrelated, the total system performance can be approximated by a root sum square (RSS) of the effect of all the individual perturbations and the design residual (Φ_0):

$$\Phi = \sqrt{\Phi_0^2 + \sum_{i=1}^n \left(\left(\frac{\Delta\Phi}{\Delta x_i} \right) (\Delta x_i) \right)^2}. \quad (1)$$

In our case, each x_i corresponds to a different degree of freedom. The sensitivity is defined as the change in performance criteria ($\Delta\Phi_i$) divided by the amount of perturbation that caused that change, Δx_i :

$$\text{Sensitivity} = \Delta\Phi_i / \Delta x_i \quad (2)$$

In general, because the system performance is calculated by RSS, the change in performance criteria ($\Delta\Phi_i$) should be calculated using a root difference squared:

$$\Delta\Phi_i = \sqrt{(\Phi(x_i + \Delta x_i))^2 - \Phi_0^2}. \quad (3)$$

However, if the nominal merit function (Φ_0) is relatively small, as wavefront errors typically are, then one can calculate the sensitivity using a linear difference, as in the following equation:

$$\frac{\Delta\Phi_i}{\Delta x_i} = \frac{\Phi(x_i + \Delta x_i) - \Phi_0}{\Delta x_i} \cong \frac{\Phi(x_i + \Delta x_i)}{\Delta x_i}. \quad (4)$$

For this analysis, the nominal criterion was significant ($\Phi_0 = \sim 15\mu\text{m}$) compared to the effect of the perturbation and we calculated the change using a root difference squared.

2.2 Perturbation analysis

Finding the effect of small perturbations for many degrees of freedom can be a time-consuming process. Fortunately, Zemax has an automatic tolerance procedure to make the process faster. Since tolerancing is not a simple process, it is not recommended to blindly trust the numbers that are output until some verification ensures that there are no errors in the testing parameters (e.g. the degrees of freedom, optimization merit function, performance criteria, and actual surfaces being toleranced). This verification can be done by perturbing the appropriate degree of freedom by a small amount, setting the compensators as variables, choosing the correct merit function, then optimizing the system and checking the resulting performance metric. Also at this time, it is a good idea to check that the perturbation is large enough for the effect to be seen clearly above the noise, but not so large that the sensitivity becomes nonlinear. For this example, perturbations that doubled the spot size were found to be appropriate.

Finding the sensitivities using a script with the automatic tolerance procedure is efficient when many different designs or combinations of compensators need to be tested. In Zemax, each row of the tolerance data editor is set for a different perturbation degree of freedom. The inverse increment sensitivity analysis (a Zemax tolerancing routine) was run with the incremental change to be the value of the nominal field-averaged rms spot size. This is an iterative procedure where Zemax decreased the values of the perturbations until the value of the criteria (the spot size) is doubled. Once the spot size was doubled for each operand, the resulting Zemax data was saved as a text file. It is possible to do the sensitivity analysis without a tolerance script, but the tolerance script conveniently records exactly which compensators and merit function are used in a text file.

The compensators, or the degrees of freedom that are the variables during the optimization procedure, should directly correspond to the degrees of freedom used for correction of the system during operation. In operation, it is optimal to adjust only the minimum number of degrees necessary to provide sufficient correction in order to keep the control system simple. The sensitivities with just one compensator (the axial position of the wide field corrector relative to the primary mirror) were found, but they were very large which would require challenging tolerances. Including more compensators allows for better optimization, so another case with five compensators was tested. These five degrees of freedom were the rigid body motions of the entire WFC (including the focal plane) that can be controlled by a hexapod structure during operation: axial position, x and y decenter and tip/tilt (about the prime focus). The sixth degree of freedom, rotation about the optical axis, is not necessary due to rotational symmetry. An important source of error is the mechanical limitation on the precision of the compensating motions. No additional compensators are used to find the sensitivities on these degrees of freedom.

2.3 Sensitivity calculations and assigning tolerances

The text file saved from the Zemax tolerancing procedure contains the value of the change Δx_i for the perturbation of each operand along with the new value of the figure of merit $\Phi(x_i + \Delta x_i)$ and the nominal figure of merit value, Φ_0 . However, the actual sensitivities ($\Delta\Phi_i/\Delta x_i$) are not calculated by Zemax. A MATLAB script was written to load the data file from Zemax, extract the necessary data and calculate the sensitivities.

Once all of the sensitivities are known, the next step is to choose tolerances that will allow the system to meet the specification. The effect of a degree of freedom on the final performance of the system can be determined by:

$$\text{Effect} = \Delta\Phi_i = (\Delta\Phi_i/\Delta x_i) * \Delta x_i = \text{Sensitivity} * \text{Tolerance}. \quad (5)$$

The RSS of the effects for all of the degrees of freedom is a reasonable approximation of total system degradation due to perturbations. A spreadsheet was set up to calculate the effect of each operand from the sensitivities and observe how changes in the tolerances affect the system. At this time, we tighten tolerances with a large effect and loosen tolerances with a small effect as much as possible. This requires close cooperation with the mechanical designers.

Table 1 shows the alignment sensitivities of the HET WFC design using five compensators defined earlier and the sensitivities of the compensator degrees of freedom (with no additional compensators).

Table 1: Sensitivities and tolerances for the HET WFC. (These tolerances are used for the Monte Carlo analysis later.)

<i>i</i>		Sensitivity [$\mu\text{m}/\mu\text{m}$ for rms spot radius MF] $\Delta\Phi_i/\Delta x_i$	Tolerance [μm] Δx_i	Effect [μm] $\Delta\Phi_i$	Notes
0	Nominal Performance			15.22	
<i>Element Alignment Tolerances</i>					
	Thermal Changes	0.0070 $\mu\text{m}/\text{ppm}$	300 ppm	2.10	All spaces except between M4 and M5
1	M2 to M3 axial spacing	0.0077	400	3.08	
2	M2 to M5 axial spacing	0.0128	100	1.28	
3	M4 to M5 axial spacing	0.1574	25	3.94	Includes thermal changes
4	M2 x or y decenter	0.0132	50	0.66	
5	M3 x or y decenter	0.0335	50	1.68	
6	M4 x or y decenter	0.3781	25	9.45	
7	M4 M5 x or y decenter	0.0309	50	1.55	
8	M2 x or y tilt	0.0211	50	1.06	across 1m diameter*
9	M3 x or y tilt	0.0382	50	1.91	across 1m diameter*
10	M4 x or y tilt	0.3535	25	8.87	across 300mm diameter*
11	M4 M5 x or y tilt	0.0172	50	0.86	across 1m diameter*
12	Focal plane axial position	0.0004	1000	0.40	
13	Focal plane x or y decenter	0.0049	250	1.23	
14	Focal plane x or y tilt	0.0213	50	1.07	across 232mm diameter*
<i>All mirrors move together (without the focal plane)</i>					
15	x or y decenter	0.0049	250	1.23	
16	x or y tilt	0.0083	250	2.08	Tilt about M2 (1m diameter)*
<i>Compensator adjustment resolution</i>					
17	Distance M1 to WFC/FP	0.8313	10	8.31	
18	x or y Decenter of WFC/FP	0.0412	10	0.41	
19	x or y Tilt of WFC/FP	0.5479	10	5.48	across 1m diameter*

*The tilts for all of the elements are assumed to be about the mirror vertex and the amount of the tilt is defined as microns displacement across a given diameter (listed in the table), which is near to the actual mirror diameter.

The system is very sensitive to the alignment of both M4 and M5. During initial phase of the sensitivity analysis, both mirrors were found to have high sensitivities which would require many tight tolerances. Instead of having two elements with very tight tolerances individually, it was found that you could have very tight tolerances for one element relative to the system (M4) and loose tolerances for the other if you ensure that the pair moves together (see rows $i = 7,11$).

2.4 Monte Carlo simulation

After the tolerances were chosen, a Monte Carlo analysis was done to show that the expected optical performance would meet the specification. In a Monte Carlo simulation, a large number of trial optical systems are created, using random perturbations, allowed by the tolerances. In general, this is a useful method for estimating statistics on the expected performance. However, it was especially important for this system because the sensitivities were found using a different criterion than the actual specification. The tolerances were chosen based on the spot size sensitivity for five field points, which was the most straightforward way to create a merit function for optimization during tolerance analysis, from which a single number criterion for evaluating system performance was calculated. The actual specification is in terms of the 80% encircled energy (EE) diameter across the field. Figure 2 shows the expected confidence levels in the encircled energy diameters based on the alignment tolerances in Table 1. Each of the degrees of freedom were perturbed to some value within the allowed tolerances using a uniform distribution. After the system is optimized and the ideal compensator motions were found, the actual compensator motions were each perturbed by a random value allowed by their tolerances. This was to simulate the limited compensator adjustment resolution, but it was found to not significantly affect spot size.

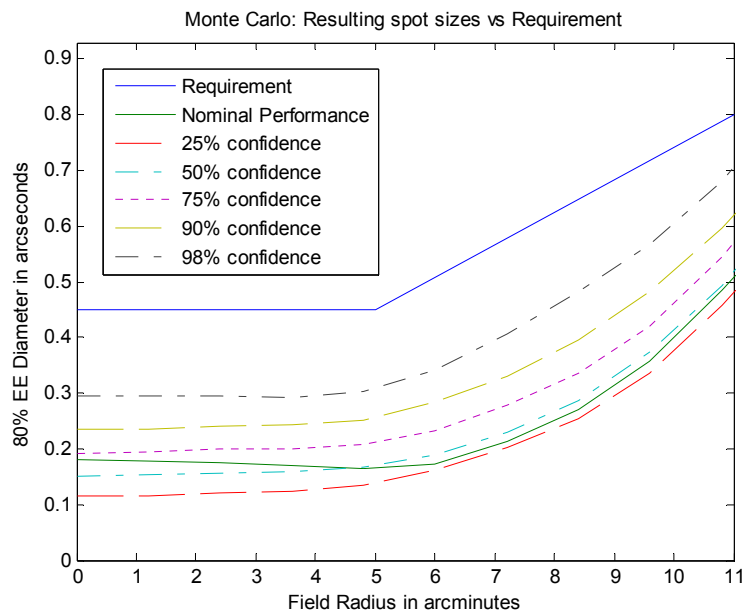


Figure 2: The results of the Monte Carlo simulation show the distribution of image sizes over many systems that meet the required tolerances in Table 1. The Requirement shown on the graph is for the overall system which includes errors other than alignment. The confidence level contours are defined by the cumulative probability for each field point.

Some misalignments may improve the spot size relative to the nominal design for field angles in one direction at the expense of increasing the spot size in other directions. The percent confidence curves are calculated by examining the field points in all of the Monte Carlo trials. Thus, one can not conclude that 25% of the trials were better than nominal, and the original design was not optimized correctly. Figure 2 does not include degradation due to other effects, such as polishing or support errors. When these other effects are included, the expected performance is still shown to meet the specification as well as a more ambitious goal specification, not shown.

A sensitivity analysis was performed to find the effect of misalignments in the HET WFC. These sensitivities helped us chose the alignment tolerances needed for the system to achieve its specifications. Many of the tilt and decenter tolerances were chosen to be 50 μm . However, we discovered that the alignment of M4 is critical to achieving the image quality specification and requires tighter tolerances of 25 μm . These tolerances help dictate the type of mechanical

structure that would be required to hold the mirrors. For example, the structure needs to be very stiff and have low thermal expansion between M4 and M5. The tolerances can also help define the type of alignment scheme that would be required while assembling the optical system. Mirrors with looser tolerances can probably be aligned by mechanical methods, such as a laser tracker or an alignment telescope, while the mirror with the tighter tolerance will require an optical test, which could be performed with a computer generated hologram (CGH). Once the alignment plan is chosen, a more detailed analysis should be performed.

3. ORTHOGONAL ABERRATION MODES

The sensitivity analysis described in Section 2 is a useful way to estimate the performance of a system for a set of given tolerances. However, it does not offer any insight to the type of aberration modes that a system may acquire due to misalignments. Finding a set of orthogonal aberration modes is the first step necessary in understanding what the misalignments are capable of doing to an optical system and can be found by using the technique of singular value decomposition (SVD) on the alignment sensitivity matrix. The alignment sensitivities found in this section are to the Zernike coefficients across the field resulting from perturbing each of the individual degrees of freedom of the four mirrors. The SVD of this sensitivity matrix also gives the combination of mirror misalignments that cause these orthogonal aberrations and the coupling between the magnitude of the misalignments and the aberrations. This section describes the process of finding the orthogonal aberration modes using the SALT Spherical Aberration Corrector (SAC) as an example. The SVD of the sensitivity matrix can also be used to formulate a least squares estimation of the alignment problem in the presence of noise. This information can also be helpful while choosing the most effective degrees of freedom to be used as compensators during the alignment phase as explained by Chapman and Sweeney.⁸

3.1 Field-dependent aberrations and the alignment sensitivity matrix

Perturbation of the alignment degrees of freedom in the corrector causes field-dependent aberrations. The alignment sensitivity matrix is a record of the Zernike aberration coefficients across the field for all of the possible misalignments. The size of the sensitivity matrix M is 384 rows by 18 columns. The alignment sensitivities were found by using MATLAB to control the perturbations of the optical design in Zemax. The connection between these programs was enabled by a MATLAB toolbox and Zemax Extensions.⁹

Each of the columns in the sensitivity matrix corresponds to a different misalignment. For the numerical simulation, it does not matter which misalignments are chosen. It could simply be one vertex tilt and one decenter in each direction or it could be any linear combination of these (4 degrees of freedom \times 4 mirrors = 16 misalignments). The primary mirror position is not perturbed since it only affects pointing. The misalignment motions used here are rotations about the center of curvature of the mirror surface and coma-free rotations. These degrees of freedom correspond well to the actual tests of the optical surfaces and are each a combination of a vertex tilt and decenter. The coma-free rotation is the appropriate combination of tilt and decenter for an individual mirror that does not cause any coma to be added to the on-axis field in the system. Also, each mirror was tilted in both x and y directions, due to the asymmetry of the pupil. The 16 different tilts of the four mirrors describe the possible motions of the system. However, since the tilt of the entire SAC is a separate degree of freedom able to be used for correction, this tilt about the point in the center of the hole in M3 was also included in the alignment sensitivity matrix to bring the total of misalignments tested to 18.

The rows of the sensitivity matrix contain the Zernike coefficients for all of the field points under consideration. The sensitivities of eight Zernike coefficients were recorded. These included focus, astigmatism, coma, trefoil and spherical aberration. The aberrations caused by misalignments usually have a constant or linear dependence on the field, so 48 field points in a grid ensured oversampling. Eight coefficients recorded for each of 48 field points resulted in 384 rows in the sensitivity matrix M . The sensitivities to each of the Zernike polynomials over all the field points for all of the misalignments is too unwieldy to list in this paper and would not provide any useful insight into the system anyway. However, the following sections describe a way to investigate the problem further.

3.2 Singular value decomposition of alignment sensitivity matrix

In addition to calculating the alignment sensitivity matrix M , MATLAB was also used to perform the singular value decomposition of the matrix and then examine the results. The singular value decomposition is a linear algebra technique to break a single matrix into three matrices as given by the following equation:

$$M = USV^T . \quad (6)$$

U and V are column orthogonal matrices and S is a diagonal matrix, where each one gives useful information about the system. Overall, they tell you which aberrations can be produced and are listed from easiest to produce (largest aberration for the smallest misalignment) to hardest to produce, and what combination of misalignments cause these different sets of orthogonal aberrations. For example, the 1st aberration mode, given by the 1st column vector from U , has some strength given by the 1st singular value from S and is formed by the configuration of misalignments given by the 1st vector in V . This is true in general for all of the column vectors in U and V :

$$M\vec{V}_i = S_i\vec{U}_i. \tag{7}$$

Each of the columns in the U matrix (384×384) is a singular vector which lists the Zernike aberrations across each of the 48 field points. Each particular resulting combination of field-dependent aberrations is an aberration mode. Since U is a column orthogonal matrix, each aberration mode is orthogonal. That is, combinations of the aberration modes uniquely describe all the possible aberrations that can result from misalignments of the SAC. (Only the first 18 columns or modes, which correspond to the 18 nonzero singular values, are important.) To visualize the aberration modes, the aberration coefficients across the field can be used to plot the wavefront maps across the field. In this system, the first two modes are constant coma across the field in the x and y directions. The Zernike coefficients from the first two columns of U (selected for a grid of nine field points out of the original 48) are plotted in Figure 3.

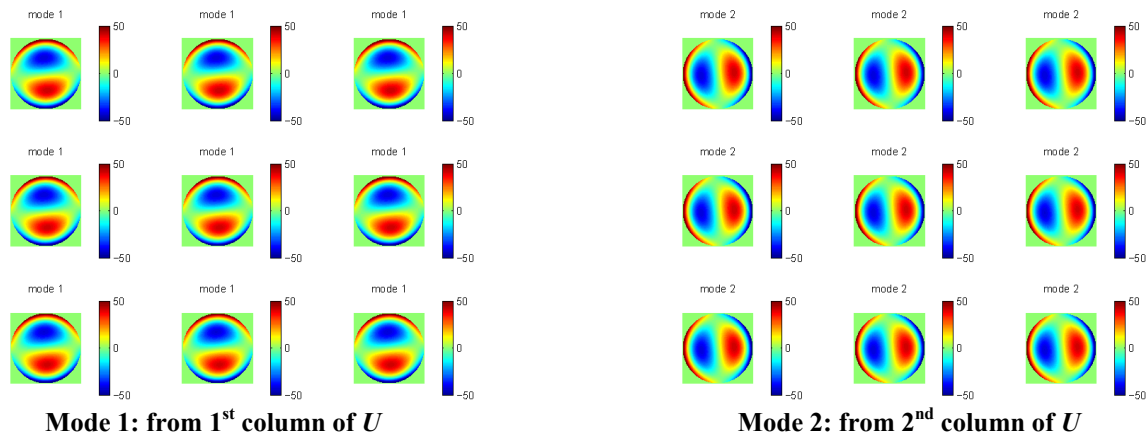


Figure 3: A visual representation of the coefficients in the first two column of the U matrix shows the first two orthogonal modes are constant coma in the x and y directions. (The center field point in the 3x3 grid is the on-axis point and the others are at either ±2.83 arcminutes (corners) or ±3 arcminute field angles.)

The other modes continue to show up in pairs and are displayed in the following section.

The S matrix (384×18) is a diagonal matrix which contains the singular values, so there are 18 total singular values. The singular values are a measure of the sensitivity of the system to a particular aberration and are always real and positive. The most sensitive aberration mode has the largest singular value. It is listed first and is followed by the other modes in order of decreasing sensitivity, as shown in Figure 4. The ratios between the singular values tell you how sensitive the measurements need to be to detect the higher order modes. This gives the required signal to noise ratio of the measurements. The modes corresponding to the lower index singular values are both easily produced by misalignments, and fixed. This is because they are easy to measure and require small adjustments.

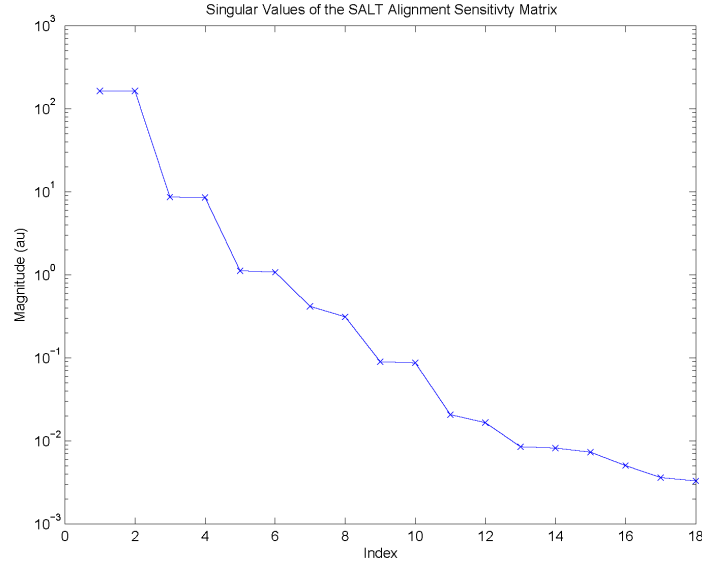
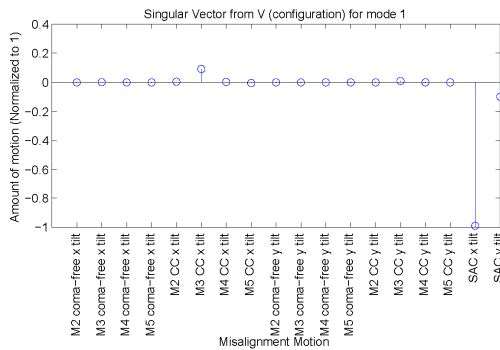
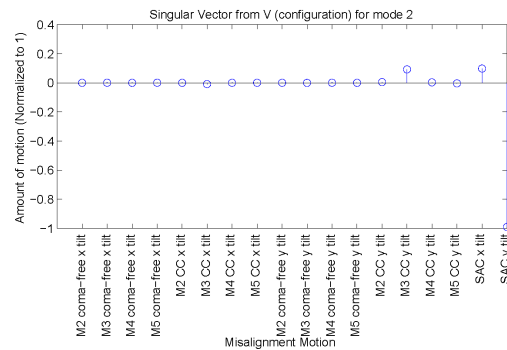


Figure 4: Singular values of the SALT SAC alignment sensitivity matrix (from the S matrix). The orthogonal aberration modes that occur in pairs have nearly identical singular values, as seen by the step-like shape.

The V matrix (18×18) describes the misalignments required to generate the orthogonal aberration modes in the U matrix. Each column of V is a singular vector for a different mode, while each row in V tells you the misalignment of a degree of freedom. The degrees of freedom are two coma-free tilts (in x and y) and two center of curvature rotations (in x and y) for each mirror M2-M5, plus the overall tip/tilt of the SAC. Figure 5 describes the source of the coma in modes 1 and 2 (observed earlier) as combination of rotation about the center of curvature of M3 in and tip/tilt of the entire SAC assembly. This makes sense because the tracker is used to correct for coma in the actual system.



Mode 1: 1st column of V



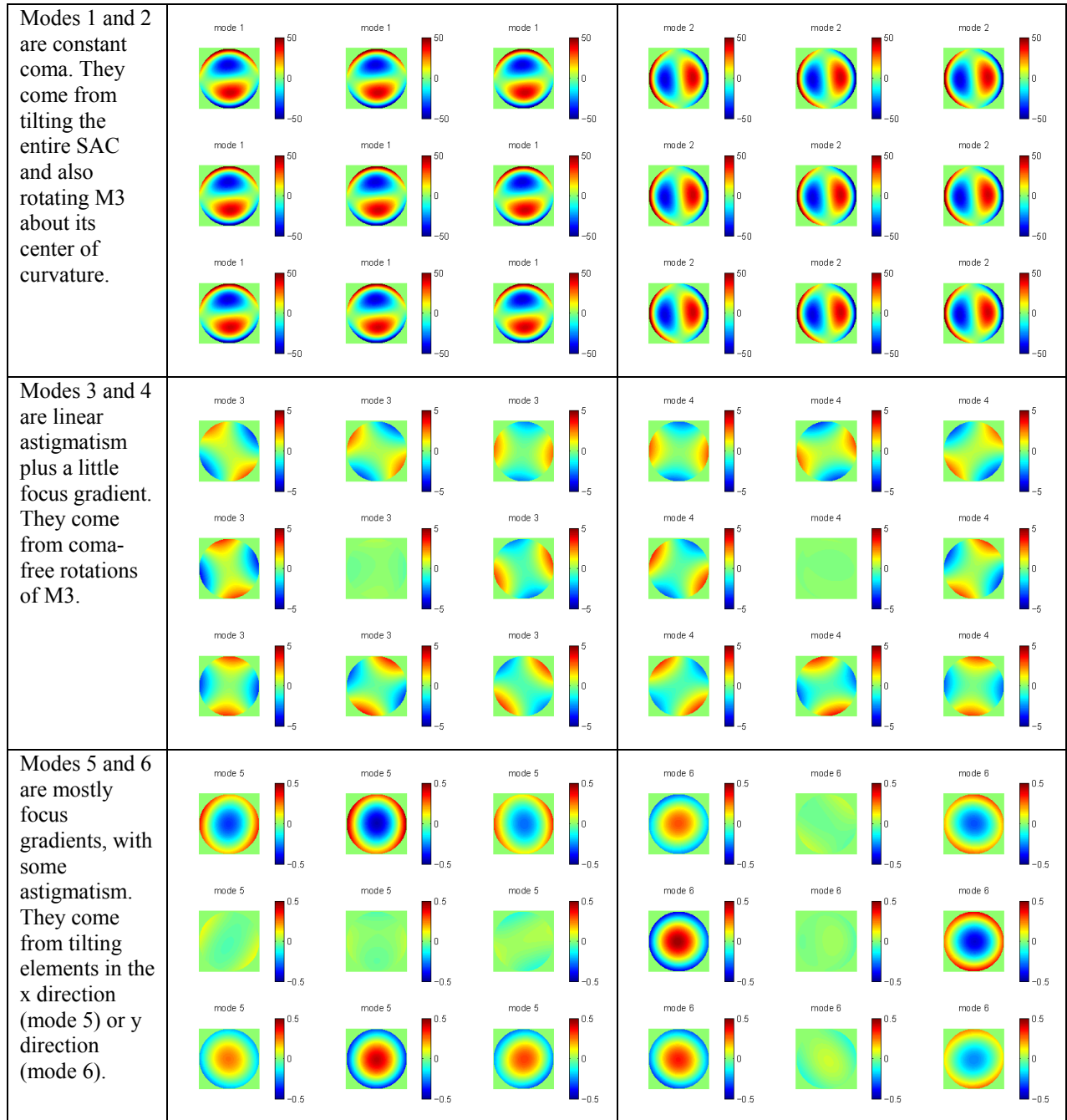
Mode 2: 2nd column of V

Figure 5: A graphical representation of the first two columns of the V matrix. This linear combination of motions causes the first two orthogonal modes of constant coma shown above in Figure 3.

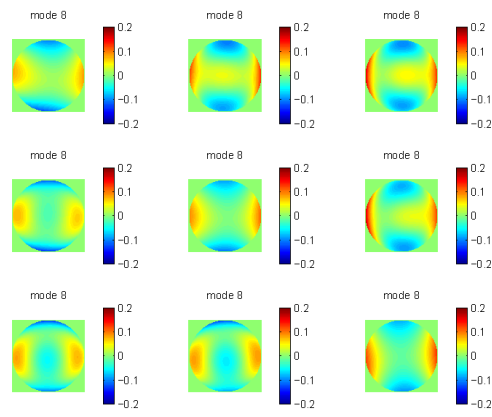
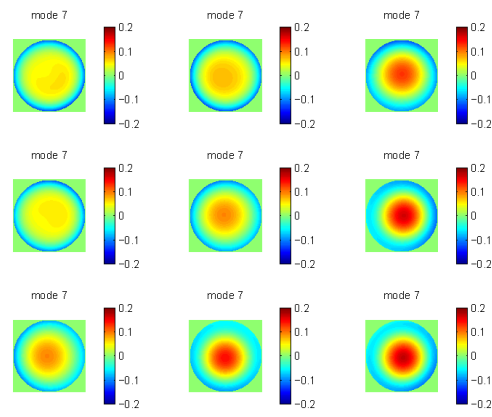
3.3 The orthogonal aberration modes of the corrector

All of the aberration modes of the corrector are displayed in Table 2. Each of the aberrations, shown for nine points in the field, are scaled by their singular values to show the amount that results from one unit of total misalignment. One can see that the amount of aberration caused by misalignment becomes increasingly smaller for higher order modes. Approximately the first twelve modes have well-behaved, low-order field dependence, and the higher order modes appear noisy.

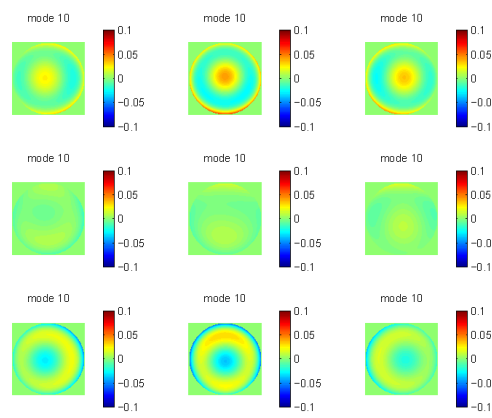
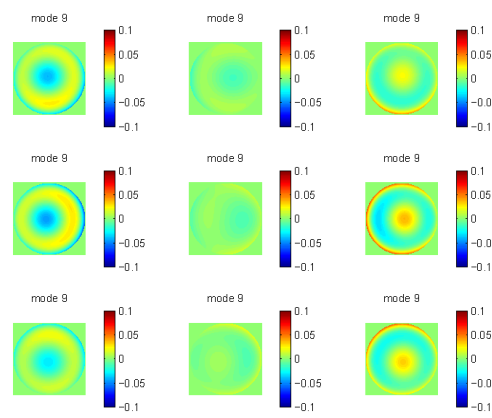
Table 2: The orthogonal aberration modes of the spherical aberration corrector are a visual representation of the coefficients in the columns of the U matrix.



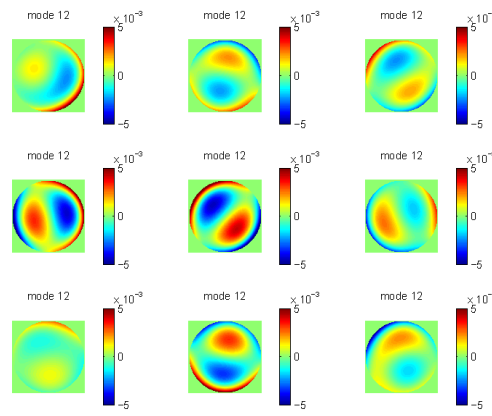
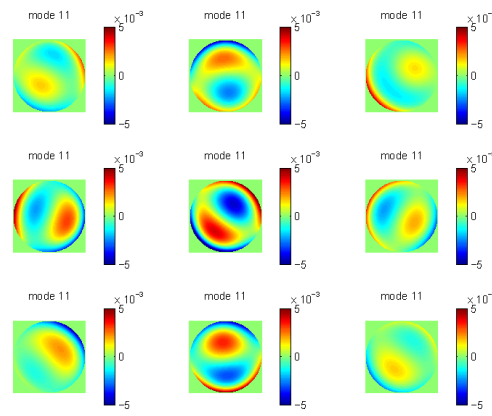
Mode 7 is mostly constant focus while mode 8 is mostly constant astigmatism. They come from a combination of all of the misalignments.

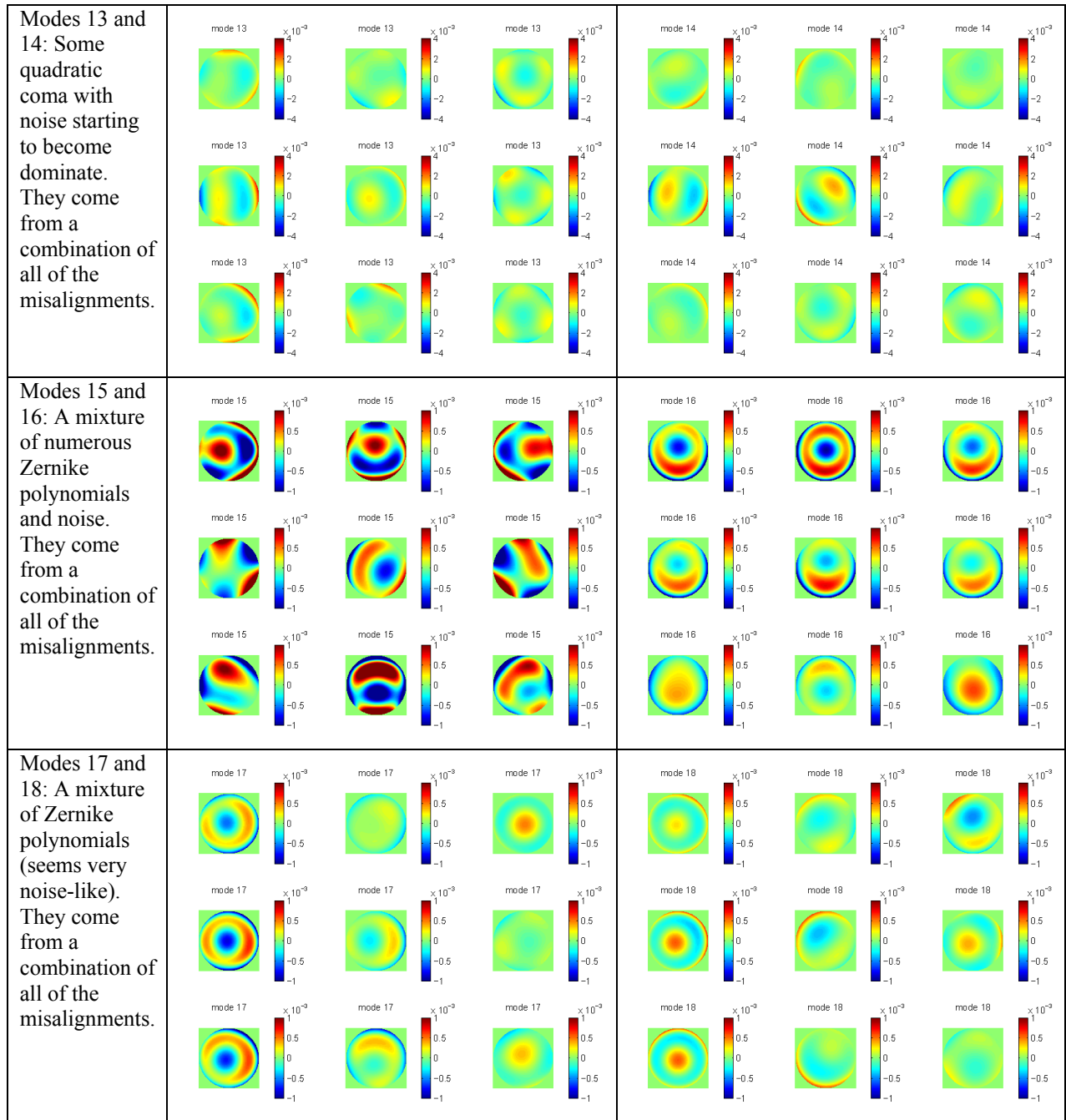


Modes 9 and 10: A mixture of multiple aberrations, dominated by spherical aberration. They come from a combination of all of the misalignments.



Modes 11 and 12: Quadratic coma, plus a constant coma offset. They come from a combination of all of the misalignments.





3.4 Orthogonal aberration modes and alignment

Measuring the Zernike aberrations across the field using wavefront sensors will give the “real life” aberration of the system. A least squares fit of the observed aberration coefficients to a number of the aberration modes can be performed. If all of the modes are included in the fit, then this is the same as a least squares solution of the alignment sensitivity matrix. Including all the modes in the least squares fit is not ideal, especially when the matrix has singular values that are very close to zero. This means that all the modes, even the ones that are noisy and not very sensitive to compensator motions are used in the fit, resulting in larger less-effective compensator motions. Fewer aberration modes can likely be used to achieve a reasonable alignment solution with smaller total motion. However, this method may require a small

adjustment to each of the 18 different degrees of freedom. This is probably more labor-intensive than desired. Chapman and Sweeney,⁸ discuss reducing the number of compensators according to the SVD.

4. CONCLUSIONS

When evaluating complicated optical systems, an understanding of the coupling between component misalignments and their effect on system performance is crucial. In this paper, two different types of analyses of alignment of four mirror aberration correctors are presented. The sensitivity analysis helps with assigning mechanical tolerances and in predicting system performance. The SVD analysis provides insight to the aberration modes the system is capable of creating through misalignments.

5. ACKNOWLEDGMENTS

We would like to thank HET and SALT for allowing us the opportunity to study their four-mirror spherical aberration corrector designs.

REFERENCES

- [1] Booth, J. A., MacQueen, P. J., Good, J. M., Wesley, G.L., Hill, G. J., Palunas, P., Segura, P. R., and Calder, R. E., "The wide field upgrade for the Hobby-Eberly Telescope," Proc. SPIE 6267, 62673W (2006).
- [2] Jungquist, R. K., "Optical design of the Hobby-Eberly Telescope Four Mirror Spherical Aberration Corrector," Proc. SPIE 3779, 2-16 (1999).
- [3] Ramsey, L.W., Sebring, T. A., and Sneden, C., "The Spectroscopic Survey Telescope Project," Proc. SPIE 2199, 31-40 (1994).
- [4] O'Donoghue, and D., Swat, A., "The Spherical Aberration Corrector of the Southern African Large Telescope (SALT)," Proc. SPIE 4411, 72-78 (2002).
- [5] Stobie, R., Meiring, J. G., and Buckley, D. A. H., "Design of the Southern African Large Telescope (SALT)," Proc. SPIE 4003, 355-362 (2000)
- [6] O'Donoghue, D., "The Correction of Spherical Aberration in the Southern African Large Telescope (SALT)," Proc. SPIE 4003, 363-372 (2000).
- [7] Dierickx, P., Brunetto, E. T., Comeron, F., Gilmozzi, R., Gontte, F. Y. J., Koch, F., le Louarn, M., Monnet, G. J., Spyromilio, J., Surdej, I., Verinaud, C., and Yaitzkova, N., "OWL phase A status report", Proc. SPIE 5489, 391-406 (2004).
- [8] Chapman, H. N., and Sweeney, D. N., "A Rigorous Method for Compensator Selection and Alignment of Microlithographic Optical Systems," Proc. SPIE 3331, 102-113 (1998).
- [9] Griffith, D., "ZEMAX DDE Toolbox for MATLAB Version 2," <http://www.mathworks.com/matlabcentral/fileexchange/loadFile.do?objectId=7507&objectType=File> (2005).